Journal of Petroleum Exploration and Production Technology (2022) 12:2785–2799
https://doi.org/10.1007/s13202-022-01481-6

ORIGINAL PAPER-PRODUCTION ENGINEERING

Investigation of the enhanced oil recovery potential of sodium cocoyl alaninate: an eco-friendly surfactant

Bennet Nii Tackie-Otoo[1,2] · Mohammed Abdalla Ayoub Mohammed[1,2] · Esther Boateng Owusu[3]

Received: 27 August 2021 / Accepted: 2 March 2022 / Published online: 14 March 2022

Abstract

Amino acid-based surfactants (AASs) and other novel surfactants have recently gained attention to provide a favorable environmental image ("green") in surfactant application. Yet their potential in enhancing oil recovery is not well investigated. Only a few works have been reported on their potential enhanced oil recovery (EOR) application with less satisfactory results. Here in, sodium cocoyl alaninate (SCA), an acylated amino acid with excellent properties that facilitate its application in other fields, is investigated for its EOR potential. Its effectiveness in lowering the interfacial tension and the emulsifying crude oil–brine mixture were studied. The ability to alter rock surface wettability and its adsorption behavior on the sand surface were studied as well. Then, its oil recovery potential was confirmed through a core displacement experiment. All studies were performed in comparison with conventionally deployed sodium dodecyl sulfate (SDS). The critical micelle concentrations for SCA (CMC = 0.23 wt%) and SDS (CMC = 0.21 wt%) were close, which serves as a good basis for comparing their EOR potential. SCA proved to be more effective in IFT reduction attaining a minimum IFT of 0.069 mN/m (i.e., ~ 98.8% IFT reduction) compared to 0.222 mN/m of SDS (i.e., ~ 96.2% IFT reduction) at the same concentration. Salinity showed a synergistic effect on the interfacial properties of both SCA and SDS but had a more significant impact on SDS interfacial properties than SCA due to low salt tolerance of SDS. The low IFT attained by SCA yielded enhanced emulsion formation and stable emulsion both at 25 °C and 80 °C for a period of one week. SCA also altered quartz surface wettability better via reduction of contact angle by 94.55% compared to SDS with contact angle reduction of 87.51%. The adsorption data were analyzed with the aid of various adsorption isotherm models. The adsorption behavior of SCA and SDS could be best described by the Langmuir model. This means a monomolecular surfactant layer exists at the aqueous–rock interface. SDS also exhibited more severe adsorption on the sand surface with the maximum adsorption density of 15.94 mg/g compared to SCA with the maximum adsorption density of 13.64 mg/g. The core flood data also confirmed that SCA has a better oil recovery potential than SDS with an additional oil recovery of 29.53% compared to 23.83% of SDS. This additional oil recovery was very satisfactory compared to the performance of other AAS that have been studied. This study therefore proves that SCA and other AAS could be outstanding alternatives to conventional EOR surfactants owing to their excellent EOR potential in addition to their environmental benign nature.

Keywords Chemical EOR · Amino acid-based surfactant · IFT reduction · Wettability alteration · Emulsification

Abbreviations

ASS	Amino acid-based surfactants
CMC	Micelle concentration
EOR	Enhanced oil recovery
O/W	Oil-in-water emulsion
SCA	Sodium cocoyl alaninate
SDS	Sodium dodecyl sulfate
SME	α-Sulfofatty acid methyl esters
W/O	Water-in-oil emulsion
XRD	X-ray diffraction
XRF	X-ray fluorescence

✉ Bennet Nii Tackie-Otoo
bennet_17006974@utp.edu.my

✉ Mohammed Abdalla Ayoub Mohammed
abdalla.ayoub@utp.edu.my

[1] Petroleum Engineering Department, Universiti Teknologi PETRONAS, 32610 Bandar Seri Iskandar, Perak Darul Ridzuan, Malaysia

[2] Centre of Research in Enhanced Oil Recovery, Universiti Teknologi PETRONAS, 32610 Bandar Seri Iskandar, Perak, Malaysia

[3] University of Mines and Technology, Tarkwa, Ghana

Parameters

c_i	Initial adsorbate concentration in aqueous solution (mg/L)
k_H	Linear isotheral model constant (L/m_2)
k_L	Langmuir constant (L/mg)
q_{max}	Maximum adsorption capacity (mg/g)
k_F	Freundlich constant (adsorption capacity)
n	Freundlich constant (adsorption intensity)
k_T	Equilibrium binding constant
B	Temkin constant
q_e	Adsorption density
Γ_m	Maximum surface excess concentration
a_m^s	Minimum surface area per molecule

Introduction

In tertiary oil recovery, one of the most practical and efficient ways of mobilizing trapped oil and stabilizing the displacement front is chemical flooding (Mandal 2015). Chemicals injected are either alkalis, surfactants, polymers, nanoparticles or their combinations (Gbadamosi et al. 2019). Among these chemical agents, surfactants prove to be very efficient in improving oil recovery through IFT reduction and wettability modification. Various laboratory experiments and field applications substantiate the feasibility and success of surfactant flooding and other surfactant-augmented flooding (Olajire 2014). A tremendous amount of research works have been conducted to design several surfactants for various conditions and applications (Negin et al. 2017). However, a primary significant concern in every surfactant application, including pharmaceuticals and cosmetics, is the low biodegradability of conventionally deployed surfactants and their incompatibility with the environment (Morán et al. 2004; Chandra and Tyagi 2013).

A newer group of surfactants that are based upon renewable raw materials have attracted attention in recent years owing to their high biodegradability, compatibility with the environment and outstanding surface properties. These include α-sulfofatty acid methyl esters (SMEs), acylated amino acids (amino acid-based surfactants) and Nopol alkoxylates (Rosen and Kunjappu 2012). In EOR studies, SME synthesized from different kinds of vegetable oil have been investigated. They exhibited superb surface activity and great potential in improving oil recovery (Kumar and Mandal 2017; Kumar et al. 2017; Pal et al. 2017, 2018, 2019; Saxena et al. 2017, 2019a). However, AAS has not been well investigated in terms of EOR application (Tackie-Otoo et al. 2020). The results of the few AAS studied on their possible EOR application are less satisfactory in comparison with the conventional counterpart.

AAS is formed by reacting the amino group of amino acids with fatty acid usually under the form of an acyl chloride (Infante et al. 2004; Morán et al. 2004). They have good tolerance to hardness and high salinity (Zhang et al. 2013). The amino acid moiety determines the main differences in adsorption and aggregation behavior among different AASs. They are either anionic, cationic, nonionic or zwitterionic based on the free functional groups. Their properties could be fine-tuned to fit specific applications through modification of the free functional groups (Morán et al. 2004). Therefore, their design could be tailored to improve their performance in improving oil recovery. Nevertheless, amino acids acylation with fatty acid chlorides in the alkaline aqueous medium after Schotten–Baumann reaction yields sodium salts of a mixture of N^{α}-acylamino acids and fatty acids (Rondel et al. 2009; Zhang et al. 2013). Rondel et al. (2009) reported that these AASs have comparable or even better performance than commercially available petroleum-based surfactants.

In this regard, the focus of this study is to investigate commercially available AAS anticipated to have comparable performance to conventional surfactants. The EOR potential of sodium cocoyl alaninate (SCA) is therefore studied. SCA is a sodium salt of an amide that is developed by reacting fatty acids chloride from coconut oil with alanine (Burnett et al. 2017). Its molecular structure is presented in Fig. 1. As an ASS, its environmental friendliness is derived from its high biodegradability through decomposition into amino acids and fatty acids. These products are common in food, and hence, the surfactant is deemed to be less toxic (Kamimura 1973; Shida et al. 1973, 1975; Kubo et al. 1976). It has been used in personal care products, household detergent and industrial cleaning agents (SAAPedia; Rondel et al. 2009; Tripathy et al. 2018). In this study, crude-oil aqueous IFT reduction capability and the ability to alter the wettability of sandstone surfaces are investigated. The emulsifying power, as well as adsorption behavior on the sand surface, is also studied. The oil recovery potential is then confirmed through core displacement experiments.

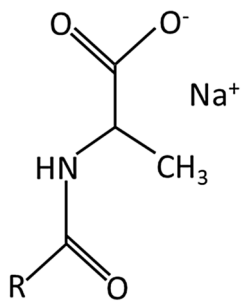

Fig. 1 Structure of SCA (R: coco group)

Experimental

Materials

The details of the various materials used in this study are summarized in Table 1. The study utilized two anionic surfactants as the primary materials for the study. Synthetic brine was prepared using nine salts. The brine composition and properties are presented in Table 2. A light crude oil from a Malaysian oil field was deployed as the oleic phase. Its composition and properties are also summarized in Table 2. The chemicals were used as received, and deionized water was not purified further. Preparation and dilution of surfactant solutions and brine were done with deionized water.

Berea sandstone cores were used for the core displacement experiments. An outcrop from a Malaysian sandstone formation was utilized for the wettability alteration and static adsorption studies. Thin slices of the rock sample with dimensions 20×20×3 mm were made and trimmed for contact angle measurements. Part of the rock was crushed and ground for batch experiments. The ground rock sample had an average particle size of 180.57 µm measured with Horiba LA-960 using laser diffraction. The composition of the crushed rock sample was determined through X-ray fluorescence (XRF) using Bruker S8 Tiger and X-ray diffraction (XRD) using PANanalytical X'Pert^3 Powder & Empyrean. The results of the XRF and XRD presented in Table 3 and

Table 1 Details of experimental materials

Materials	Purity	Supplier
Sodium cocoyl alaninate	~28–30%	Skyrun Industrial Company Ltd (China)
Sodium dodecyl sulfate	Over 85%	Merck Chemicals
Strontium chloride hexahydrate, $SrCl_2{\cdot}6H_2O$	AR, 99%	Merck Chemicals
Calcium chloride dihydrate, $CaCl_2{\cdot}2H_2O$	AR, 99.5%	R and M chemicals (Malaysia)
Magnesium chloride hexahydrate, $MgCl_2{\cdot}6H_2O$	AR, 99.5%	R and M chemicals (Malaysia)
Potassium chloride, KCl	AR, 99.5%	R and M chemicals (Malaysia)
Sodium chloride, NaCl	AR, 99.5%	R and M chemicals (Malaysia)
Barium chloride dihydrate, $BaCl_2{\cdot}2H_2O$	AR, over 99%	R and M chemicals (Malaysia)
Sodium bicarbonate, $NaHCO_3$	AR, over 99%	R and M chemicals (Malaysia)
Sodium sulfate, Na_2SO_4	AR, over 99%	R and M chemicals (Malaysia)
Iron (III) chloride, $FeCl_3$	97%	R and M chemicals (Malaysia)
Crude oil	–	Portray (M) SDN BHD

Table 2 Brine and crude oil composition and properties

Salt	Concentration (g/L)	Crude oil composition	% weight
NaCl	8.4526	Saturates	24.6
KCl	0.4048	Aromatics	14.5
$MgCl_2{\cdot}6H_2O$	0.5299	Resins	16.3
$CaCl_2{\cdot}2H_2O$	0.1713	Asphaltenes	44.6
$SrCl_2{\cdot}6H_2O$	0.0011		
$BaCl_2{\cdot}2H_2O$	0.0018		
$FeCl_3$	0.0024		
Na_2SO_4	3.6358		
$NaHCO_3$	0.8028		

Properties	Brine	Crude oil
Density (g/mL) @ 25 °C	1.0069	0.8404
Density (g/mL) @ 80 °C	0.98097	0.809
Viscosity (mPa.s) @ 25 °C	0.75	13.6
Viscosity (mPa.s) @ 80 °C	0.4638	6.3
Salinity (mg/L)	1400.5	
Total acid number (mg KOH/g)		0.01

Table 3 Composition of sandstone sample

Elemental composition	Concentration (%)	Oxide	Concentration (%)
Si	44.5	SiO_2	95.2
Ca	1.21	P_2O_5	1.87
P	0.818	CaO	1.69
Fe	0.363	Al_2O_3	0.554
Al	0.293	Fe_2O_3	0.519
K	0.118	K_2O	0.142
Cu	0.0066	CuO	0.0082
Sr	0.0024	SrO	0.0029

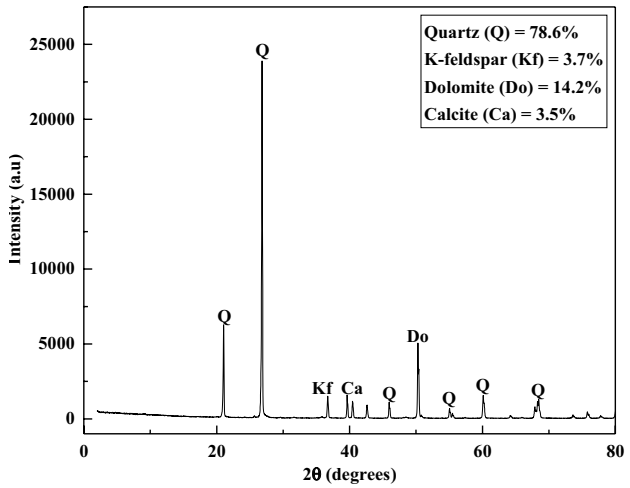

Fig. 2 XRD pattern of sandstone outcrop

Fig. 2, respectively, showed that silica or quartz is the predominant component of the sandstone outcrop.

Surface tension measurements

The surface tensions of the various surfactant solutions at the different concentrations were measured with Kruss DSA 25 at ambient conditions. For the surface tension measurement, a 1.825-mm-diameter needle was used to suspend drops of the surfactant solutions in the air medium. Profile fitting of the suspended droplet was then made deploying the pendant drop method using Advance 1.4 software in the tensiometry mode. Single measurements were taken repeatedly to ensure that the values were reproducible. The subsequent analyses were made using the mean of these values. The surface tension measurements were first validated by measuring the surface tension of deionized water at ambient conditions. The value was 74.37 mN/m, which agrees with values from open literature. The uncertainty in measurements is estimated to be between 0.05 and 0.5 mN/m.

Conductivity measurements

Electrical conductivity measurements of various surfactant solutions at different concentrations were taken with conductivity meter; Eutech Con 450 at ambient conditions. Surfactant stock solutions were gradually diluted with deionized water to achieve the concentration variation. Before conductivity measurement, the diluted solution is stirred for a while and left to settle. Conductivity readings are recorded after they are stable for about a minute. Continuous recording is made till readings become consistent. Further analyses were then done using the mean of consistent values. The uncertainty in measurements is estimated to be 0.1 μS/m.

Interfacial tension measurements

The IFT between crude oil and the various aqueous solution of surfactants was measured using the spinning drop tensiometer (SVT 20, Data physics) at room temperature. The measurement process involves the injection of the aqueous phase into a fast exchange capillary tube. The capillary tube is then first set to rotate at very low rotational speed (100–300 rpm); then, crude oil droplet is injected. The low rotation during the crude oil droplet injection is to prevent the oil droplet from sticking to the walls of the capillary tube. The tube is then set to rotate at 5000 rpm which causes the oil droplet to stretch. The elongated oil droplet is profile fitted using the SVT 20 software. The dynamic IFT was recorded at a 20-s interval until equilibrium was reached. The interfacial property in this study is based on the equilibrium IFT. To avoid interference from the former solution, the fast exchange capillary tube is cleaned with toluene, followed by acetone and deionized water to remove and crude oil and surfactant residues. The IFT between crude oil and deionized water at ambient conditions was 5.82 mN/m.

Emulsion stability test

Emulsification is mostly the prevalent mechanism in surfactant oil recovery processes. Therefore, the emulsifying power of the surfactants and emulsion stability was also studied. The emulsification test involved homogenizing 1.4 wt% NaCl brine and crude oil using the surfactants at different concentrations as the emulsifying agent. The brine and crude oil were mixed at a 1:1 ratio, and homogenization was achieved using T18 digital ULTRA-TURRAX. The homogenized systems are put in 25-mL test tubes and observed over time while they disintegrate into their original component at 25 °C and 80 °C. The period of observation was one week, and the rate of disintegration was used to analyze the stability of the emulsions formed. Salt concentration was then varied, and surfactant concentration was kept constant to study the effect of salinity.

Contact angle measurements

Wettability alteration studies were done by measuring of contact angle of surfactant aqueous solution on an oil-aged rock surface. The sessile drop method was applied in measuring the contact angles using the Kruss DSA 25 at ambient conditions. The rock slices described under the material section were utilized for the contact angle measurements. Toluene and methanol were used to first clean the slices and then dried. Oil-wetness of the slices was induced by aging the slices in crude oil over a fortnight at 80 °C. Afterward, n-heptane was used to rinse the oil-aged slices and then dried. The slices' initial wetting conditions were determined from deionized water contact angle. The measurement process involved dropping surfactant aqueous solution via a needle onto the slice. The solution then forms a sessile drop on the slice, which is analyzed by the Young–Laplace fitting. The measurement is taken for 10 min. The impact of cross-contamination from traces of the previous solution was mitigated by conducting each measurement on an unaffected part of the rock slice.

Static adsorption studies

The adsorption behavior of the surfactants on the sand surface was studied through a series of batch experiments. Each experiment consists of mixing a 20-mL aqueous solution of surfactant at a particular concentration with 2 g of sand. The mixture of adsorbate and adsorbent was agitated continuously for 24 h in a water bath shaker at 120 rpm rotational speed and 25 °C temperature to attain equilibrium. The supernatant of the mixture was then decanted and centrifuged for 30 min at 3000 rpm using the Thermo Scientific Multifuge X1R Centrifuge. The centrifugation causes all suspended sand particles to gather at the bottom of the centrifuge tubes. The solution is then filtered and analyzed to determine the residual concentration. The residual concentration is determined via conductometry using the Eutech Con 450 conductivity meter at ambient conditions. The accuracy is within ± 5 μS/m.

Core flooding experiments

The final part of the study involved determining the oil recovery potential of the surfactants through core displacement experiments. The Berea sandstone cores used were first characterized to determine various properties summarized in Table 4. The core samples were then vacuum saturated in brine. The core flood experiments were conducted at 80 °C temperature and 2500 psi confining pressure. The drainage process was then mimicked by displacing the brine in the core with crude oil at 0.5 cc/min to connate water saturation. Then, brine was injected at 0.2 cc/min to residual oil saturation to mimic the waterflooding process. 0.5 PV of the surfactant solution is then injected followed by chase water at the same rate. The test is concluded when oil production ceases.

Results and discussion

Critical micelle concentration determination

The surface tension data acquired at room temperature were used to determine the critical micelle concentration (CMC) of SCA. The variation of surface tension with the concentration of SCA and SDS on a semi-log plot is shown in Fig. 3a. There is a sudden break in surface tension decline with surfactant concentration, which is followed by an increasing trend with a very gentle slope for SCA and a zero slope for SDS. The breaking point in the surface tension variation with surfactant concentration corresponds to the CMCs of the surfactants. The CMCs of SCA and SDS were determined from the conductivity data as well by William's method, as presented in Fig. 3b. In the variation of specific conductivity with surfactant concentration, the breaking point indicates the initiation of micellization (Williams et al. 1955).

From Fig. 3a, SCA has a CMC of 7.94 mM (0.23 wt%) while SDS has a CMC of 7.41 mM (0.21 wt%). The closeness of their CMC could be attributed to their molecular structure. With regard to their hydrophobic group, SCA's cocoyl group is a mixture of acyl groups with different chain lengths (Zhang et al. 2013). The preponderate group is lauroyl, which means SCA has a chain length of 12 carbons or more. Therefore, SCA likely has a lower CMC than SDS because the micellization process is facilitated with increasing straight-chain hydrophobic length. However, SCA's hydrophilic group, which is alaninate, contains a carboxyl group as well as a secondary amino group (Bordes

Table 4 Properties of Berea sandstone core samples

Core sample no.	Dry weight (g)	Diameter (cm)	Length (cm)	Porosity (%)	Pore volume (cc)	Permeability (mD)	
						K_{air}	K_{∞}
Core A	141.93	3.815	5.821	15.23	10.14	169.87	162.26
Core B	195.58	3.814	8.021	15.13	13.60	164.06	154.74

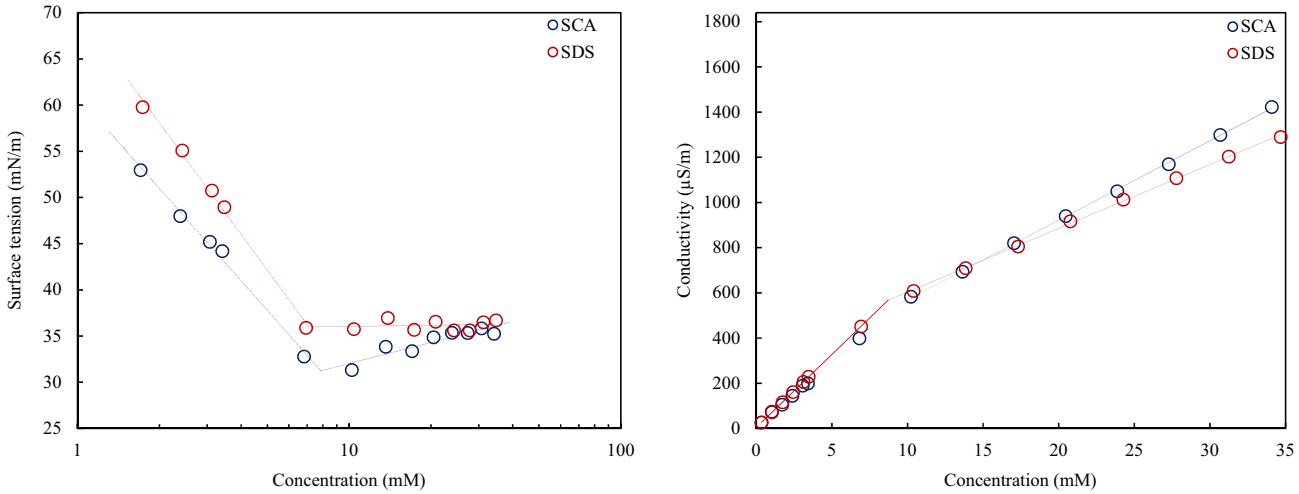

Fig. 3 CMC determination by surface tension (left) and conductivity (right) method at 25 °C

and Holmberg 2015). The amide bond increases the water solubility of the unimer substantially (Bordes et al. 2010), which delays micellization. These opposing effects explain the similarity of their CMCs. It could also be deduced from Fig. 3a that SCA proves to be slightly more surface active than SDS predominantly due to the mixed alkyl chain length. Figure 3b also shows that SCA has a CMC of 9.5 mM (0.28 wt%) and SDS has a CMC of 8.7 mM (0.25 wt%). The CMC variation agrees with the surface tension method only that values are a bit higher due to the difference in the method of determination. The closeness of the CMC of SDS to SCA means their EOR potential could be compared since comparable surfactant concentrations could be used.

Interfacial tension reduction

A prerequisite for the displacement of the residual crude oil in rock capillaries is ultra-low IFT. The interfacial properties of SCA were, therefore, analyzed using data acquired from the spinning drop tensiometer. This equipment has the precision for measuring such ultra-low values. The equilibrium IFT values at different concentrations for SCA at ambient conditions are presented in Fig. 4 in comparison with that of SDS. Due to the closeness in their CMCs, a comparable trend is observed. The equilibrium IFTs decrease significantly with increase in surfactant concentration to a minimum after which a gentle increase in the IFT with concentration variation is observed. The surfactant concentration at which the minimum IFT is attained corresponds to the CMCs of the surfactants. The reduced CMC values for the IFT measurements compared to the surface tension and conductivity method could be due to the crude oil components that could affect the

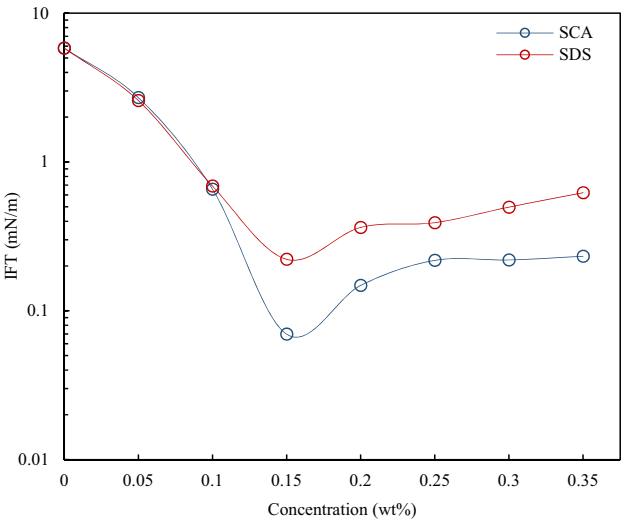

Fig. 4 Crude oil–aqueous solution equilibrium IFTs for SCA and SDS at 25 °C

micellization process. An imperative observation from Fig. 4 is the superior interfacial activity exhibited by SCA over SDS. The mixture of hydrophobic chain length is the major factor for this superiority in the interfacial property of SCA (Gang et al. 2020). From our previous studies, SDS adsorbs more effectively onto surface and interfaces compared to SCA and that should have yielded a better interfacial property (Tackie-Otoo and Mohammed 2020). SCA attained a minimum IFT of 0.069 mN/m, which is not ultra-low. However, it is reported in the literature that IFT values in this range (i.e., 10^{-2}) yield stable emulsions (Hezave et al. 2013). This is confirmed in the emulsification studies presented in the next section.

Effect of salinity

Salinity has a significant impact on interfacial properties. Generally, salt yields a synergistic effect with surfactants in reducing IFT (Pal et al. 2018; Saxena et al. 2019a). The effectiveness of IFT reduction is directly related to the effectiveness and efficiency of adsorption of surfactant molecules on the oil–water interface, which is measured by the maximum surface excess concentration (Γ_m). For ionic surfactant, the addition of salt causes an increase in the ionic strength, which decreases the thickness of the ionic atmosphere around the head groups of the surfactants. This phenomenon yields tighter packing at the oil–water interface and increase in the Γ_m, therefore leading to improved IFT reduction (Rosen and Kunjappu 2012).

The effect of salt addition on the two surfactants is shown in Fig. 5. Both surfactants exhibited improved IFT reduction upon the addition of salt. IFT is reduced until an optimum salinity beyond which IFT either remains constant or increases. Comparing the performance of the two surfactants in the presence of salt, SDS showed superior IFT reduction to SCA. SDS achieved an optimum salinity of ~ 3 wt% NaCl with IFT value of ~ 0.02 mN/m beyond which the IFT remained constant. SCA, on the other hand, exhibited a significant IFT reduction at 1% NaCl concentration. Beyond this salt concentration, IFT kept reducing but the reduction is subtle. Surfactants are usually most effective when near the point of minimum solubility in the solvent in which they are dissolved, since they are most surface active at this point (Rosen and Kunjappu 2012). SCA has a higher salt tolerance (~ 29 wt%) than SDS (~ 7 wt%) (Tackie-Otoo and Mohammed 2020). Therefore, with SDS close to its minimum solubility in this salinity range, it is expected to have superior interfacial property to SCA.

Effect of temperature

As expounded earlier under the salinity effect, the IFT reduction capabilities of surfactants are best explained based on their effectiveness and efficiency of adsorption onto the oil–water interface. According to Rosen and Kunjappu (2012), for ionic surfactants, temperature increase causes a decrease in adsorption effectiveness and efficiency. This observation could be ascribed to improved solubility of surfactant molecules at elevated temperatures, limiting the concentration of surfactant molecules at the oil–water interface. Nevertheless, the literature has reported contradicting findings on IFT response to temperature (Karnanda et al. 2013). As reported by Pal et al. (2018), IFT is observed to decrease further with temperature increase. Authors explained that increase in temperature causes an increase in the number of available adsorption sites due to increased interfacial curvature.

The IFT variations with temperature for SCA and SDS are presented in Fig. 6. As observed from this figure for both surfactants, a decreasing trend is first observed in IFT with increasing temperature to a minimum; then, an increasing trend is observed with further increase in IFT. This observation has been explained to be due to distribution of surfactant between the oil and water and emulsion inversion from oil-in-water (O/W) at low temperature to water-in-oil (W/O) at high temperature (Ye et al. 2008). The temperature at which the minimum IFT is achieved is therefore called the phase inversion temperature (PIT). At surfactant concentration of 0.075 wt%, SCA attained a PIT of 50 °C with corresponding minimum IFT of 0.566 mN/m, while SDS attained

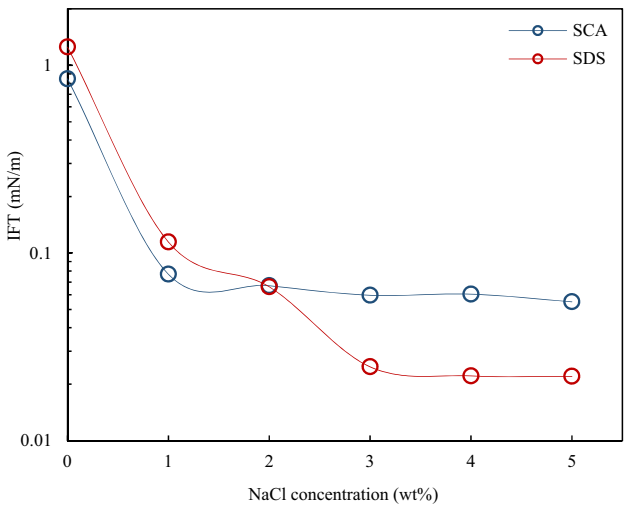

Fig. 5 Salinity effect on IFT at 0.075 wt% surfactant concentration at 25 °C

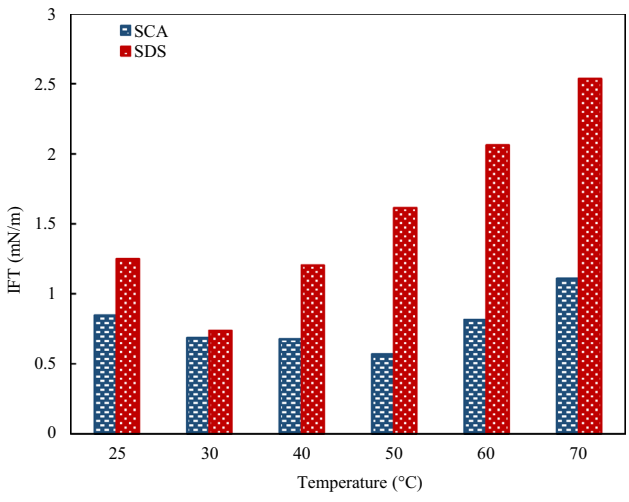

Fig. 6 Effect of temperature on IFT at 0.075 wt% surfactant concentration

a PIT of 30 °C with minimum IFT of 0.7 mN/m. Therefore, when only a decreasing or an increasing trend is observed, then the temperature range is below or above the PIT. It is worth mentioning that the IFT of SCA was far lower than SDS at high temperature.

Emulsification studies

To substantiate the IFT results and the effect of salinity and temperature on the interfacial properties of SCA, emulsification studies were conducted at different surfactant concentrations (0.05–0.25 wt%), 1.4 wt% NaCl concentration and two temperatures (25 °C and 80 °C). The formation of stable emulsion requires the IFT between oil and water to be low, and adequate shear must be used to facilitate the homogenization (Scott et al. 1965). Aqueous solutions of surfactants and electrolyte were mixed with the crude oil at 5000 rpm for 10 min. Figure 7 shows the emulsion formed after an hour of settling time. Firstly, it is observed from Fig. 7 that the emulsion volume diminishes with surfactant concentration. This observation confirms the IFT variation with surfactant concentration as constant shear is applied (Bryan and Kantzas 2009). That is sufficient reduction in IFT improves the emulsification process. Therefore, the observed emulsification behavior could be attributed to the fact that the presence of salt facilitates micellization and shifts the CMC to a lower concentration. Our previous work on surface activity confirms that the addition of salt depresses the CMC of SCA to 0.05 wt% (Tackie-Otoo and Mohammed 2020). Therefore, the emulsifying power of the surfactant decreases beyond this concentration due to increase in IFT. This observation also confirms that the amount of surfactant required in the emulsion-based EOR would be much lower compared to conventional surfactant flooding (Saxena et al. 2019a). SCA proved to have better emulsifying power than SDS, and this is attributed to the superior interfacial property of SCA as explained under IFT reduction capability.

Further studies involved investigating the effect of salinity on the emulsifying power of the surfactants. Figure 8 shows the images of the emulsification behavior of surfactants at 0.05 wt% concentration with different concentrations of NaCl (1–5 wt%) obtained after 1 h of settling time. Both surfactants formed significant volume of emulsion at the various salt concentrations. The emulsification behavior at different salt concentration corroborates the effect of salinity of the interfacial behavior of the surfactants. The volume of emulsion formed by SCA did not vary much with salt

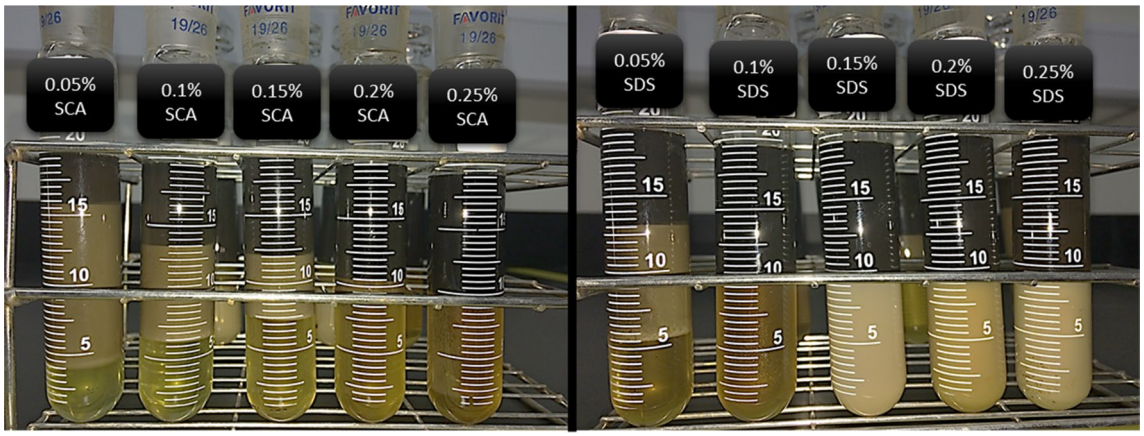

Fig. 7 Emulsification by SCA and SDS after 1 h of settling time at 80 °C

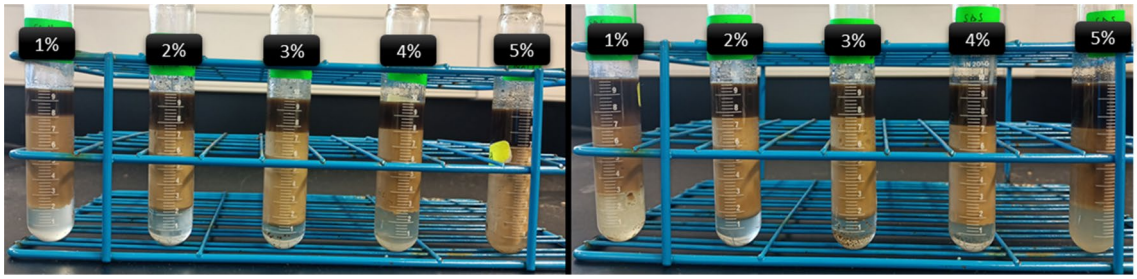

Fig. 8 Emulsion salinity scan of SCA (left) and SDS (right) at 80 °C obtained after 1 h

concentration as IFT reduction had a subtle variation with salt concentration. On the other hand, the volume of emulsion formed by SDS increased through a maximum then decreased with increasing salt concentration. This observation confirms the IFT variation, which decreases to a minimum after which no significant variation is observed with increasing salt concentration. It is also observed that the increase in salt concentration may lead to inverting the emulsion type from O/W emulsion to W/O emulsion. This observation was obvious in the emulsions formed by SDS but not those formed by SCA. With 1:1 oil–water ratio, the emulsion type is derived from the quantity of oil and water emulsified. The addition of strong electrolyte to O/W emulsion decreases the electrical potential on the dispersed particles and increases the interaction between the surfactant ions and counterions making them less hydrophilic (Rosen and Kunjappu 2012). As explained, the salinity range tested affects SDS ions more than SCA.

Emulsion stability

The emulsion stability is inferred from the phase volume ratio variation observed for one week as presented in Fig. 9. The observation is made at room temperature and 80 °C to investigate the effect of temperature on emulsion stability. The rate of emulsion disintegration depicts that the emulsions formed are more stable at lower temperature than higher temperature. At high temperature, IFT between the

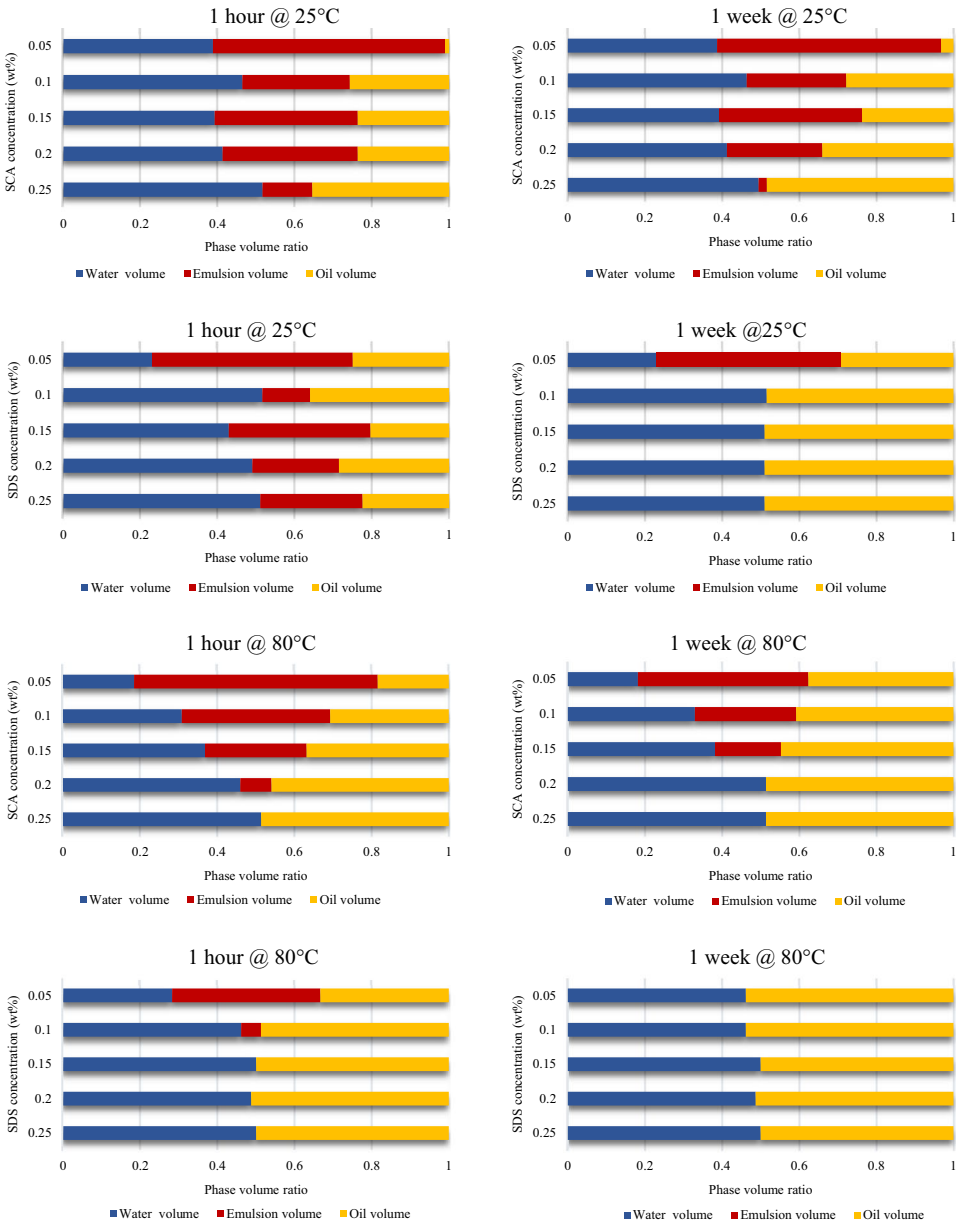

Fig. 9 Emulsion stability of SCA and SDS at the various concentrations at 25 °C and 80 °C

two phases increases as shown under IFT reduction. This phenomenon is due to improved solubility of surfactants reducing their surface activity. The viscosity of the phases reduces and thermal agitation of the dispersed phase occurs as well (Sjoblom 2005; Rosen and Kunjappu 2012). Temperature increase results in increased vapor pressure, which causes increased flow of molecules through the interface. All these phenomena reduce emulsion stability with temperature increase. It is also apparent in Fig. 9 that most of the emulsions formed at low temperature are W/O emulsion, while at high temperature, O/W emulsions are formed. As explained by Rosen and Kunjappu (2012), some emulsions stabilized by ionic surfactants may invert to W/O upon temperature reduction.

The stability of the emulsions formed by SCA is also compared to that of SDS. At room temperature, none of the emulsions formed by SCA full disintegrated after the one week of observation. On the other hand, all the emulsions formed by SDS disintegrated except for the system with 0.05 wt% SDS. At 80 °C, after an hour of settling time, only the 0.25 wt% SCA system completely disintegrated. Most of the SDS systems, on the other hand, completely disintegrated except for the systems with 0.005 wt% and 0.1 wt% SDS. All the emulsions of the SDS systems disappeared by the one-week period of settling, but the SCA systems proved to form stable emulsions. This observation could be attributed to the very high IFT values of SDS systems at high temperature. Low IFT stimulates emulsion formation and also could hinder immediate recoalescence yielding stable emulsions (Opawale and Burgess 1998). It is observed from Fig. 9 that for the SCA systems, though the volume of emulsion formed diminished with concentration due to increasing IFT, the stability of the emulsion formed increases. Increasing surfactant concentration increases the quantity of surfactant molecules adsorbed on the oil–water interface improving the strength of the interface film. With higher surfactant concentration, the emulsions formed have stronger electrostatic repulsion due to anionic groups. Hence, the resistance of emulsion droplets to coalescence is increased and emulsion stability is improved (Yuan et al. 2015).

The effect of salinity on emulsions stability was tested also as shown in Fig. 10. The increase of salt concentration increases ionic strength which reduces electrostatic repulsion among the dispersed phases. This increases coalescence of the dispersed phase and hence increases the emulsion instability (Yuan et al. 2015; Rayhani et al. 2022). Nevertheless, both SCA and SDS systems at 0.05 wt% surfactant concentration formed stable emulsions irrespective of salinity in this study. As reported by Perles et al. (2012), there is an ionic strength window within which emulsion stability is improved. Beyond this window, the emulsion stability is impaired. Therefore, it could be explained that the tested salinity range with the low surfactant concentration yields ionic strength within this window, resulting in stable emulsion irrespective of salinity. The emulsification mechanism causes the oil to be entrained and produced in water. The oil droplets could also merge and block pores to improve the sweep efficiency by the emulsification and entrapment mechanism (Bryan and Kantzas 2009; Sheng 2010). Hence, the emulsifying ability of SCA proves its great potential for EOR application.

Wettability alteration studies

The spreading coefficient defined as the variation in surface free energy per unit area is a measure of the extent to

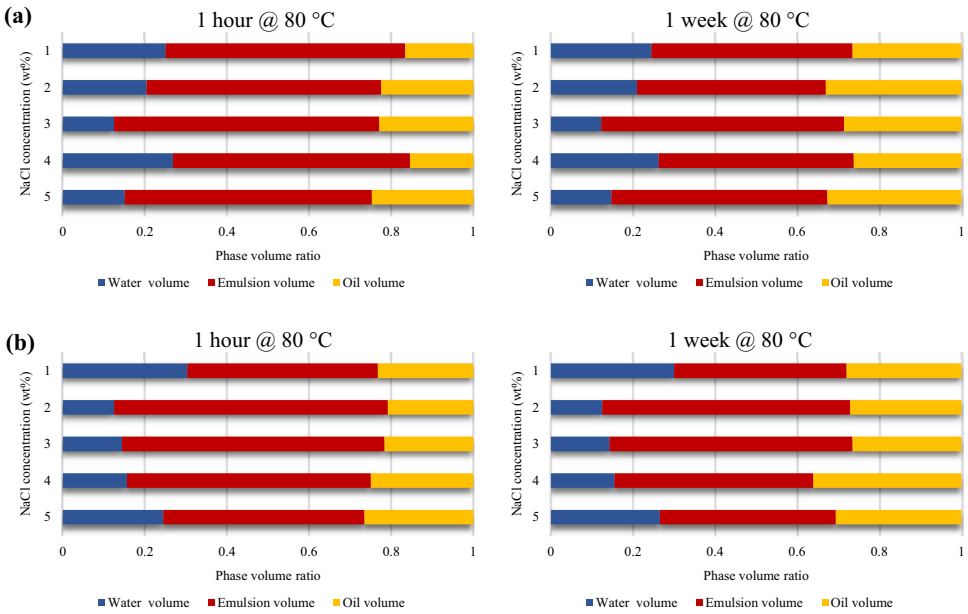

Fig. 10 Effect of salinity on emulsion stability of **a** SCA and **b** SDS at 0.05 wt% at 80 °C

which fluid could wet a surface. The spreading coefficient is a function of the surface tension of the various phases and the interfacial tension between them. Therefore, surface and interfacial tension measurements can be used to determine the wetting power of fluid (Rosen and Kunjappu 2012). Nevertheless, the surface and interfacial tensions of solids are difficult to measure. An indirect means of determining the spreading coefficient is the contact angle measurement, which is also a function to the interfacial free energies of the various phases (Zdziennicka and Jańczuk 2010; Jarrahian et al. 2012). The performance of SCA in altering rock surface wettability was therefore studied through contact angle measurements.

The final contact angles attained in 10 min by various surfactant aqueous solutions on oil-aged quartz surfaces are presented in Fig. 11. The contact angle for water on the quartz surface used for SCA was around 89° initially and 66° after 10 min. That used for SDS had an initial contact angle of 88° and a final contact angle of 61°. This observation shows that the quartz surfaces were intermediate wet. Comparing the contact angles attained by SCA and SDS at different concentrations, both surfactants exhibited excellent wetting power, yet SCA showed better wettability alteration potential over SDS. The two surfactants are anionic and are therefore expected to alter quartz surface via the ion-pair mechanism (Standnes and Austad 2000). This is a more effective wettability alteration mechanism. Nevertheless, SCA proved to be better than SDS in reducing surface and interfacial tension, which are related to the contact angle and hence the observed superiority in wettability alteration.

Adsorption behavior

Surfactant adsorption on rock surfaces has an adverse impact on surfactant EOR processes. This phenomenon leads to surfactant loss that reduces the quantity of surfactant available to improve oil recovery. To ensure optimum surfactant flooding process, the adsorption phenomenon has to be considered in the designing of surfactant formulations. Static adsorption studies usually give overestimated adsorption densities. Nevertheless, it is widely deployed in research work due to its simplicity. The batch experiments were performed to find the quantity of surfactant adsorbed per unit adsorbent mass. The plots of adsorption density against the initial surfactant concentration for SCA and SDS are presented in Fig. 12.

It could be seen that SDS exhibits severe adsorption compared to SCA. This is due to the effectiveness of adsorption. Depending on the orientation of the surfactant molecules on the adsorbent, the effectiveness of adsorption may be affected or not affected by the hydrophobic group of the surfactant. If the molecules adsorb perpendicular to the absorbent, only the size of the hydrophilic head determines the effectiveness of adsorption (Rosen and Kunjappu 2012). In this study, SCA has a bulky hydrophilic head (alaninate) compared to the sulfate of SDS. Therefore, SDS has a tighter packing, and more molecules will adsorb compared to SCA. This observation agrees with their minimum surface area per molecule (a_m^s) and the maximum surface excess concentration (Γ_m) derived from the Gibbs adsorption isotherm (Rosen and Kunjappu 2012). They are measures of the effectiveness of adsorption. Their analysis is detailed in our previous publication (Tackie-Otoo and Mohammed 2020). SDS has a higher Γ_m and a lower a_m^s than SCA showing more effectiveness in adsorption.

The experimental data for the two surfactants were then modelled using various adsorption isotherms. These models are described in detail in the literature (Ahmadi and Shadizadeh 2015; Saxena et al. 2019b; Yekeen et al. 2019). The model parameters and their coefficient of determination are presented in Table 5. It is evident from Table 5 that both surfactants' adsorption behaviors follow the Langmuir model

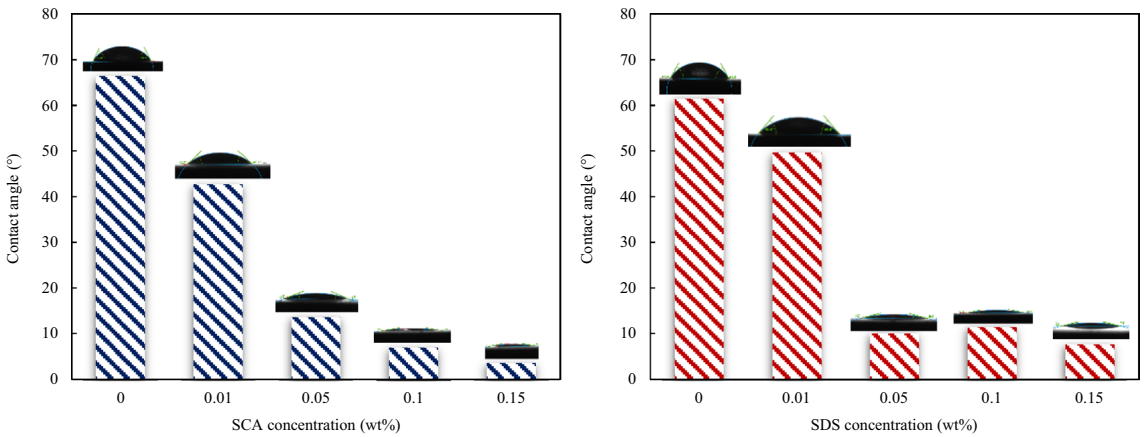

Fig. 11 Contact angle variation with concentration for SCA (left) and SDS (right) at 25 °C

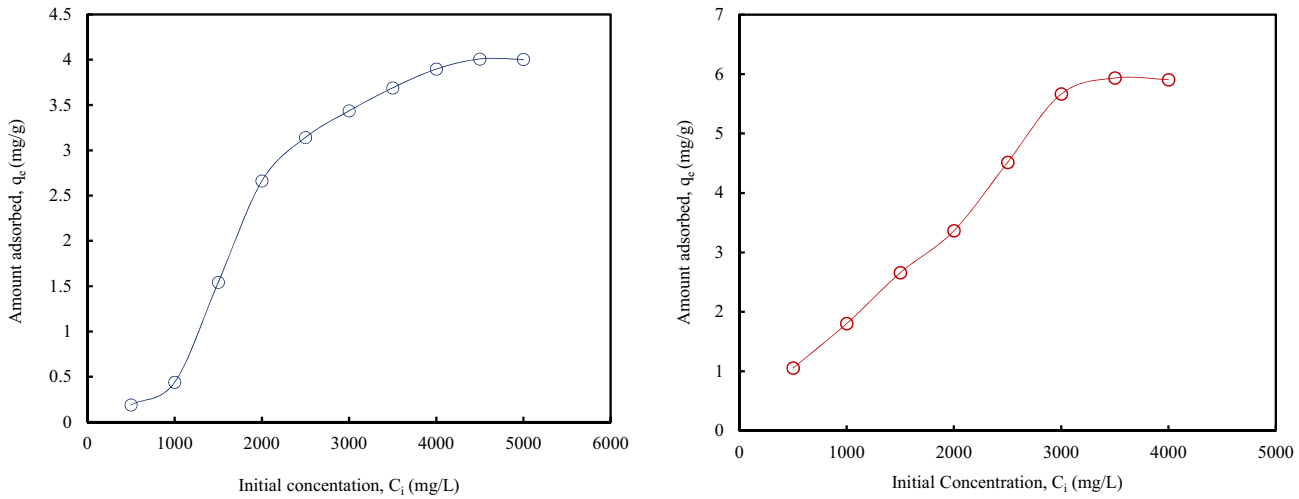

Fig. 12 Adsorption density versus initial concentration for SCA (left) and SDS (right) at 25 °C

Table 5 Summary of adsorption models' parameters for SCA and SDS solution at 25 °C

Isotherm models	SCA			SDS		
	Adsorption parameters		R^2	Adsorption parameters		R^2
Linear	$k_H = 0.0009$	$C = 0.6095$	0.792	$k_H = 0.0018$	$C = 0.4918$	0.9471
Langmuir	$k_L = 0.000265$	$q_{max} = 13.64$	0.9525	$k_L = 0.00017$	$q_{max} = 15.94$	0.9881
Freundlich	$k_F = 0.000042$	$\frac{1}{n} = 1.4103$	0.8904	$k_F = 0.0056$	$\frac{1}{n} = 1.1509$	0.9837
Temkin	$k_T = 0.0019$	$B = 1.9881$	0.9404	$k_T = 0.0029$	$B = 2.5613$	0.9171

[R^2 (SCA) = 0.9525 and R^2 (SDS) = 0.9881]. Therefore, the adsorption behaviors of the surfactants are predicted to form a monomolecular layer at the rock-aqueous interface. The maximum adsorption capacity parameters (q_{max}) also confirm that SDS adsorption on the sand surface is more severe than SCA.

Oil recovery potential

The preliminary studies presented above have shown the potential of SCA for improving oil recovery. SCA has exhibited excellent performance in IFT reduction and wettability alteration. The final step in this study is the deployment of a core displacement experiment to confirm the potential of SCA to improve oil recovery. Two core flood tests were performed for SCA using core sample B and SDS using core sample A. From the IFT and contact angle studies, 0.15 wt% was found as the optimum concentration for improving oil recovery for both surfactants. Nevertheless, a higher concentration was used to make up for chemical loss due to adsorption (Pal et al. 2018). A concentration of 0.3 wt% is therefore chosen for the flooding experiments. The results of the flooding experiments are presented in Fig. 13. It is evident from the results that both surfactants recovered additional oil after the waterflood. The recovery mechanism could be deduced from the dynamic curves. The surge in pressure drops during the chemical injection, which is followed by an abrupt reduction in water cuts, depicts emulsification and entrapment. The emulsions block the pores and cause flow diversion, which results in pressure build-up. This phenomenon creates new pathways for subsequent waterflood (Bryan and Kantzas 2009; Sheng 2010). The oil droplets are also entrained along with the aqueous flowing phase.

As observed in Fig. 13, SCA achieved a higher additional oil recovery of ~ 30% than SDS which attained ~ 24%. The observed additional recovery confirms the superior interfacial and surface activity of SCA to SDS. SCA is superior in IFT reduction as discussed in "Interfacial tension reduction" section which yielded the formation of stable emulsions. The predominant mechanism in the recovery process has been explained to be due to emulsification; hence, the formation of stable emulsions by SCA yields better additional oil recovery. SCA also proved to be better in wettability alteration than SDS, which means more favorable relative permeability condition for the SCA flooding process.

The performance of SCA in enhancing oil recovery is also compared to other AAS presented in the literature. These results are summarized in Table 6. SCA proved superior to other AAS reported in the literature (Rostami et al. 2017; Madani et al. 2019; Asl et al. 2020; Deljooei et al. 2021).

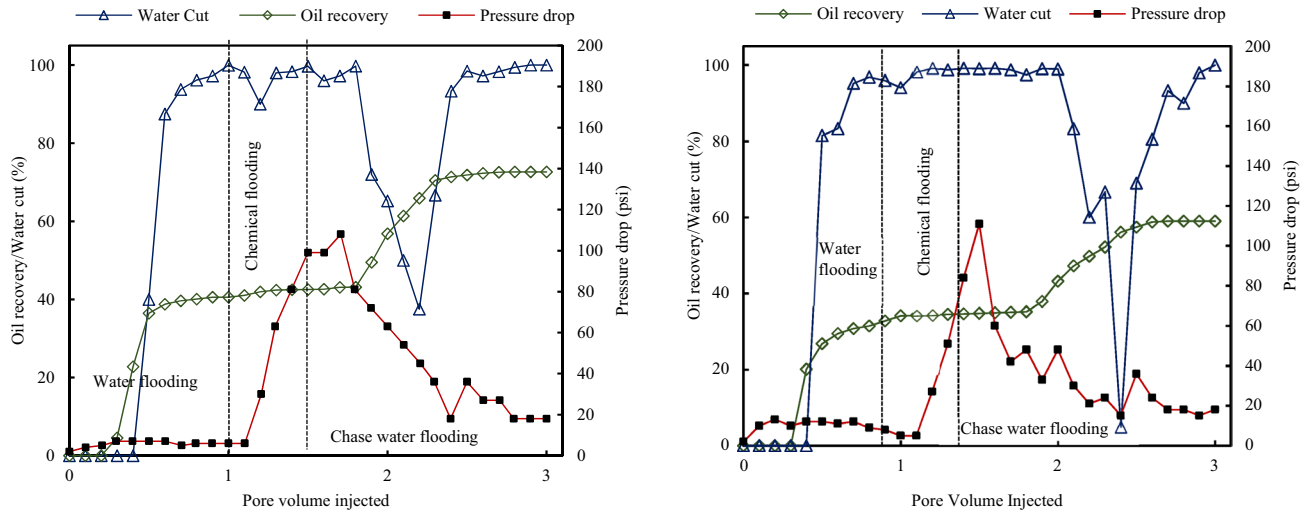

Fig. 13 Dynamics curves of core displacement experiments for SCA (left) and SDS (right)

Table 6 Core flooding results for SCA, SDS, and other AAS

Surfactant	Core type	Brine salinity (ppm)	Additional oil recovery (%OOIP)	Reference
Sodium cocoyl alaninate	Sandstone	14,000	29.53	This work
Sodium dodecyl Sulfate	Sandstone	14,000	23.83	This work
N-lauroyl-L-lysine	Carbonate	50,000	10	Rostami et al. (2017)
S-lauroyl-L-arginine	Carbonate	50,000	2.49	Madani et al. (2019)
Lauroyl arginine	Carbonate	100,000	11.9	Asl et al. (2020)
Lauroyl cysteine	Carbonate	100,000	8.9	Asl et al. (2020)
S-dodecanoyl-L-aspartic acid	Sandstone	20,000	11.19	
		40,000	6.04	Deljooei et al. (2021)

The superior performance of SCA could be attributed to the fatty acid source of its hydrophobic group. The cocoyl group is from coconut oil, which yields a mixture of fatty acids (Zhang et al. 2013). Therefore, SCA possesses a mixture of alkyl groups with different chain lengths. Hence, a better surface and interfacial property are exhibited by SCA, which leads to better additional oil recovery. The high additional oil recovery confirms its superior surface and interfacial properties over these AASs as reported in our previous work (Tackie-Otoo and Mohammed 2020).

Conclusion

In this work, SCA proved to have a great potential in enhancing oil recovery. SCA exhibited superior interfacial properties and wetting power on sandstone surface to conventionally deployed SDS. SCA also proved to have the great emulsifying ability by forming emulsions that were stable over 1 week. Adsorption studies also showed that SCA has less severe adsorption on the sand surface compared to SDS. These attributes translate into achieving additional oil recovery of 29.53% in a core displacement test. This is about 24% more than the additional recovery achieved by SDS. The other AAS reported in the literature could only achieve additional recovery in the range of 3–12%. This study on SCA, therefore, proves that there is a class of AAS that could outperform the conventional EOR surfactants or exhibit comparable performance in enhancing oil recovery while helping to deal with environmental issues associated with chemical EOR processes. Query SCA's commercial availability and its attributes to reduce environmental footprint of surfactant flooding process render it an outstanding replacement to conventional EOR surfactants.

Acknowledgements The authors would like to acknowledge and appreciate the Universiti Teknologi PETRONAS for financial assistance through YUTP Grant 015LC0-232.

Funding Funding was provided by YUTP (Grant 015LC0-232).

Declarations

Conflict of interest On behalf of all the co-authors, the corresponding author states that there is no conflict of interest.

References

Ahmadi MA, Shadizadeh SR (2015) Experimental investigation of a natural surfactant adsorption on shale-sandstone reservoir rocks: static and dynamic conditions. Fuel 159:15–26. https://doi.org/10.1016/j.fuel.2015.06.035

Asl HF, Zargar G, Manshad AK et al (2020) Experimental investigation into l-Arg and l-Cys eco-friendly surfactants in enhanced oil recovery by considering IFT reduction and wettability alteration. Pet Sci 17:105–117

Bordes R, Holmberg K (2015) Amino acid-based surfactants–do they deserve more attention ? Adv Colloid Interface Sci 222:79–91. https://doi.org/10.1016/j.cis.2014.10.013

Bordes R, Tropsch J, Holmberg K (2010) Role of an amide bond for self-assembly of surfactants. Langmuir 26:3077–3083

Bryan J, Kantzas A (2009) Potential for alkali-surfactant flooding in heavy oil reservoirs through oil-in-water emulsification. J Can Pet Technol 48:37–46

Burnett CL, Heldreth B, Bergfeld WF et al (2017) Safety assessment of amino acid alkyl amides as used in cosmetics. Int J Toxicol 36:17S-56S

Chandra N, Tyagi VK (2013) Synthesis, properties, and applications of amino acids based surfactants: a review. J Dispers Sci Technol 34:800–808

Deljooei M, Zargar G, Nooripoor V et al (2021) Novel green surfactant made from L-aspartic acid as enhancer of oil production from sandstone reservoirs: wettability, IFT, microfluidic, and core flooding assessments. J Mol Liq 323:115037

Gang H, Zhang Q, Wang W et al (2020) Synthesis and interfacial properties of bio-based zwitterionic surfactants derived from different fatty acids in non-edible vegetable oils. J Renew Mater 8:417

Gbadamosi AO, Junin R, Manan MA et al (2019) An overview of chemical enhanced oil recovery: recent advances and prospects. Int Nano Lett 9(3):171–202

Hezave AZ, Dorostkar S, Ayatollahi S et al (2013) Dynamic interfacial tension behavior between heavy crude oil and ionic liquid solution (1-dodecyl-3-methylimidazolium chloride ([C12mim][Cl]+ distilled or saline water/heavy crude oil)) as a new surfactant. J Mol Liq 187:83–89

Infante MR, Pérez L, Pinazo A et al (2004) Amino acid-based surfactants. Comptes Rendus Chim 7:583–592

Jarrahian K, Seiedi O, Sheykhan M et al (2012) Wettability alteration of carbonate rocks by surfactants: a mechanistic study. Coll Surf Physicochem Eng Asp 410:1–10

Kamimura A (1973) Colorimetric determination of long-chain N-acylglutamic acids with pinacyanol. Agric Biol Chem 37:457–464

Karnanda W, Benzagouta MS, AlQuraishi A, Amro MM (2013) Effect of temperature, pressure, salinity, and surfactant concentration on IFT for surfactant flooding optimization. Arab J Geosci 6:3535–3544

Kubo M, Yamada K, Takinami K (1976) Effects of chemical structure on biodegradation of long chain N-acyl amino acids. J Ferment Technol 54(5):323–332

Kumar A, Mandal A (2017) Synthesis and physiochemical characterization of zwitterionic surfactant for application in enhanced oil recovery. J Mol Liq 243:61–71. https://doi.org/10.1016/j.molliq.2017.08.032

Kumar S, Kumar A, Mandal A (2017) Characterizations of surfactant synthesized from Jatropha oil and its application in enhanced oil recovery. AIChE J 63:2731–2741

Madani M, Zargar G, Takassi MA et al (2019) Fundamental investigation of an environmentally-friendly surfactant agent for chemical enhanced oil recovery. Fuel 238:186–197

Mandal A (2015) Chemical flood enhanced oil recovery: a review. Int J Oil Gas Coal Technol 9:241. https://doi.org/10.1504/IJOGCT.2015.069001

Morán MC, Pinazo A, Pérez L et al (2004) "Green" amino acid-based surfactants. Green Chem 6:233–240

Negin C, Ali S, Xie Q (2017) Most common surfactants employed in chemical enhanced oil recovery. Petroleum 3:197–211. https://doi.org/10.1016/j.petlm.2016.11.007

Olajire AA (2014) Review of ASP EOR (alkaline surfactant polymer enhanced oil recovery) technology in the petroleum industry : prospects and challenges. Energy 77:963–982. https://doi.org/10.1016/j.energy.2014.09.005

Opawale FO, Burgess DJ (1998) Influence of interfacial properties of lipophilic surfactants on water-in-oil emulsion stability. J Colloid Interface Sci 197:142–150

Pal N, Saxena N, Mandal A (2017) Phase behavior, solubilization, and phase transition of a microemulsion system stabilized by a novel surfactant synthesized from castor oil. J Chem Eng Data 62:1278–1291

Pal N, Saxena N, Divya Laxmi KV, Mandal A (2018) Interfacial behaviour, wettability alteration and emulsification characteristics of a novel surfactant: implications for enhanced oil recovery. Chem Eng Sci 187:200–212. https://doi.org/10.1016/j.ces.2018.04.062

Pal N, Kumar S, Bera A, Mandal A (2019) Phase behaviour and characterization of microemulsion stabilized by a novel synthesized surfactant: implications for enhanced oil recovery. Fuel 235:995–1009

Perles CE, Volpe PLO, Bombard AJF (2012) Study of the cation and salinity effect on electrocoalescence of water/crude oil emulsions. Energy Fuels 26:6914–6924

Rayhani M, Simjoo M, Chahardowli M (2022) Effect of water chemistry on the stability of water-in-crude oil emulsion: role of aqueous ions and underlying mechanisms. J Pet Sci Eng 211:110123

Rondel C, Alric I, Mouloungui Z et al (2009) Synthesis and properties of lipoamino acid–fatty acid mixtures: influence of the amphiphilic structure. J Surfactants Deterg 12:269–275

Rosen MJ, Kunjappu JT (2012) Surfactants and interfacial phenomena. John Wiley & Sons, Hoboken

Rostami A, Hashemi A, Takassi MA, Zadehnazari A (2017) Experimental assessment of a lysine derivative surfactant for enhanced oil recovery in carbonate rocks: mechanistic and core displacement analysis. J Mol Liq 232:310–318. https://doi.org/10.1016/j.molliq.2017.01.042

SAAPedia Sodium Cocoyl Alaninate-Surfactant-SAAPedia. http://www.saapedia.org/en/saa/?type=detail&id=1358. Accessed 26 Apr 2020

Saxena N, Pal N, Dey S, Mandal A (2017) Characterizations of surfactant synthesized from palm oil and its application in enhanced oil recovery. J Taiwan Inst Chem Eng 81:343–355

Saxena N, Goswami A, Dhodapkar PK et al (2019a) Bio-based surfactant for enhanced oil recovery: interfacial properties, emulsification and rock-fluid interactions. J Pet Sci Eng 176:299–311

Saxena N, Kumar A, Mandal A (2019b) Adsorption analysis of natural anionic surfactant for enhanced oil recovery: the role of mineralogy, salinity, alkalinity and nanoparticles. J Pet Sci Eng 173:1264–1283

Scott GR, Collins HN, Flock DL (1965) Improving waterflood recovery of viscous crude oils by chemical control. J Can Pet Technol 4:243–251

Sheng J (2010) Modern chemical enhanced oil recovery: theory and practice. Gulf Professional Publishing, Texas

Shida T, Homma Y, Misato T (1973) Bacterial degradation of N-lauroyl-L-valine. Agric Biol Chem 37:1027–1033

Shida T, Homma Y, Kamimura A, MISATO T, (1975) Studies on the control of plant deseases by amino acid derivatives. v. degradation of N-lauroyl-L-valine in soil and the effect of sunlight and ultraviolet rays on N-lauroyl-L-valine. Agric Biol Chem 39:879–883

Sjoblom J (2005) Emulsions and emulsion stability: surfactant science series/61 second. crc press, Florida

Standnes DC, Austad T (2000) Wettability alteration in chalk: 2. mechanism for wettability alteration from oil-wet to water-wet using surfactants. J Pet Sci Eng 28:123–143. https://doi.org/10.1016/S0920-4105(00)00084-X

Tackie-Otoo BN, Mohammed MAA (2020) Experimental investigation of the behaviour of a novel amino acid-based surfactant relevant to EOR application. J Mol Liq 316:113848. https://doi.org/10.1016/j.molliq.2020.113848

Tackie-Otoo BN, Ayoub Mohammed MA, Yekeen N, Negash BM (2020) Alternative chemical agents for alkalis, surfactants and polymers for enhanced oil recovery: research trend and prospects. J Pet Sci Eng 187:106828

Tripathy DB, Mishra A, Clark J, Farmer T (2018) Synthesis, chemistry, physicochemical properties and industrial applications of amino acid surfactants: a review. Comptes Rendus Chim 21:112–130. https://doi.org/10.1016/j.crci.2017.11.005

Williams RJ, Phillips JN, Mysels KJ (1955) The critical micelle concentration of sodium lauryl sulphate at 25 °C. Trans Faraday Soc 51:728–737

Ye Z, Zhang F, Han L et al (2008) The effect of temperature on the interfacial tension between crude oil and gemini surfactant solution. Coll Surf Physicochem Eng Asp 322:138–141. https://doi.org/10.1016/j.colsurfa.2008.02.043

Yekeen N, Padmanabhan E, Idris AK, Ibad SM (2019) Surfactant adsorption behaviors onto shale from Malaysian formations: influence of silicon dioxide nanoparticles, surfactant type, temperature, salinity and shale lithology. J Pet Sci Eng 179:841–854

Yuan C-D, Pu W-F, Wang X-C et al (2015) Effects of interfacial tension, emulsification, and surfactant concentration on oil recovery in surfactant flooding process for high temperature and high salinity reservoirs. Energy Fuels 29:6165–6176

Zdziennicka A, Jańczuk B (2010) The relationship between the adhesion work, the wettability and composition of the surface layer in the systems polymer/aqueous solution of anionic surfactants and alcohol mixtures. Appl Surf Sci 257:1034–1042

Zhang G, Xu B, Han F et al (2013) Green synthesis, composition analysis and surface active properties of sodium cocoyl glycinate. Am J Anal Chem 85(1):445–450